RSC Advances

PAPER

View Article Online
View Journal | View Issue

Cite this: *RSC Adv.*, 2020, **10**, 14313

Highly-dispersed ruthenium precursors *via* a self-assembly-assisted synthesis of uniform ruthenium nanoparticles for superior hydrogen evolution reaction†

Xingyan Liu, *[a] Guangmei Jiang,[a] Yuwei Tan,[a] Shuang Luo,[a] Mengmeng Xu,[a] Yiming Jia,[b] Peng Lu[a] and Youzhou He*[a]

Received 13th February 2020
Accepted 23rd March 2020

DOI: 10.1039/d0ra01402h

rsc.li/rsc-advances

For the first time, highly-dispersed ruthenium precursors *via* a hydrogen-bond-driven melamine–cyanuric acid supramolecular complex (denoted CAM) self-assembly-assisted synthesis of uniform ruthenium nanoparticles with superior HER performance under both acidic and alkaline conditions are reported. Electrochemical tests reveal that when the current density is −10 mA cm^{-2}, the optimal Ru/CNO electrocatalyst could express low overpotentials of −18 mV and −46 mV, low Tafel slopes of 46 mV dec^{-1} and 100 mV dec^{-1}, in 0.5 M H_2SO_4 and 1.0 M KOH, respectively. The remarkable HER performance could be attributed to uniform ruthenium with the aid of highly dispersed ruthenium precursors (Ru–CAM) and subsequent annealing results in uniform ruthenium nanoparticles.

1 Introduction

Along with the human industrialization advancements, a large amount of natural resources, particularly energy resources, have been heavily consumed. The utilization of fossil fuels, which are still the main human energy sources, has already caused great pressures on climate change and global warming. Therefore, the development of a new and clean energy has become an urgent requirement for human society.[1] Hydrogen, as a clean and environmentally-friendly energy source, is favored as the abundant resource of high calorific value.[2] Among numerous hydrogen production processes, electrocatalytic water decomposition is an efficient method for generating hydrogen from the cathode hydrogen evolution reaction (HER).[3] Platinum-based materials, as a perfect cathode alternative, are widely researched for electrocatalytic hydrogen production due to their excellent electrocatalytic activity. However, the scarcity of platinum resources on the earth leads to a very high cost, which makes it difficult to be widely used in practical applications.[4] Therefore, scientists have turned their attention to other selectable materials that are expected to be additional alternatives with excellent electrocatalytic hydrogen evolution performance instead of the platinum-based materials.

Ruthenium (Ru), as an inexpensive alternative to Pt, has exhibited excellent Pt-like performance in electrocatalytic hydrogen production. Recently, a series of Ru-based materials with remarkable HER performances have been widely investigated.[5] Yang *et al.* have synthesized a new type of ruthenium-supported carbon nanocatalyst with carbon quantum dots (Ru@CQDs). The electrochemical test showed that Ru@CQDs has an excellent hydrogen evolution activity under alkaline conditions, which could be ascribed to the synergistic effects between ruthenium nanoparticles and carbon quantum dots.[6] Lu *et al.* prepared a Ru-based electrocatalyst that exhibited an overpotential of −12 mV at −10 mA cm^{-2} in 1 M KOH. It was found that the excellent alkaline HER activity mainly results from the atomically dispersed Ru species coordinating with the N and C atoms.[7] Despite these achievements, a simple and scalable synthesis of uniform ruthenium catalysts with excellent performance for hydrogen evolution is still a great challenge.[8] For instance, the ruthenium particles would easily agglomerate during most tedious multistep synthesis procedures, which could reduce their catalytic activities and limit practical applications.

With the aim of solving the above problems, we focused on the melamine–cyanuric acid supramolecular complex (denoted CAM), which is one novel type of co-crystal formed through a hydrogen-bond-driven self-assembly between melamine and cyanuric acid, resulting in nanorod configuration.[9] The lattice of hydrogen-bonded CAM is the perfect template on which we could design a family of self-assembled hydrogen-bonded aggregates with various single-atomic metals.[10] Nagai *et al.* have reported a facile recovery system for precious metals based

[a]*Chongqing Key Laboratory of Catalysis and New Environmental Materials, College of Environment and Resources, Chongqing Technology and Business University, Chongqing 400067, China. E-mail: xyliuctbu@126.com; yzhectbu@163.com*

[b]*Department of Chemistry "G. Ciamician", University of Bologna, Ravenna Campus, 48121 Ravenna, Italy*

† Electronic supplementary information (ESI) available. See DOI: 10.1039/d0ra01402h

on CAM, in which metal ions in an aqueous solution could coordinate to melamine with high efficiency and subsequently self-assemble with cyanuric acid through hydrogen bonds to form a precipitate of the metal–CAM complex that could be separated by filtration from the solution easily.[11] Therefore, the metal ions could uniformly distribute in the nanorod configuration of the metal–CAM complex, which gives us the idea of designing various nanorod materials with highly-dispersed single-atomic metals.

In this study, we have successfully prepared a cheap and efficient catalyst with uniform ruthenium nanoparticles through highly dispersed nanorod Ru–CAM precursors by a simple stirring-calcination method, which could make the Ru species highly-dispersed and avoid the bulk agglomeration in the following calcination process. Electrocatalytic test results show that the optimal Ru/CNO electrocatalyst exhibits exceptional HER activity under both acidic and alkaline conditions.

2 Results and discussion

As illustrated in Scheme 1, Ru/CNO are synthesized *via* a facile stirring-calcination method in which $RuCl_3 \cdot 3H_2O$ from its aqueous solution coordinates with melamine through amino groups with high efficiency at first, subsequently self-assembling with cyanuric acid through hydrogen bonds to form the metal–CAM complex (Ru–CAM) precipitation with high dispersity of ruthenium. As shown in Fig. S1(a–c),† the rod morphologies of the calcined precursors with various sizes obtained through the stirring-calcination method and hydrothermal-calcination method are different from the lumpy morphology obtained by the grinding-calcination method. We found that the Ru–CAM obtained by the stirring-calcination method is smaller in size than that obtained through a hydrothermal-calcination method, which is consistent from analysis with Brunauer–Emmett–Teller adsorption isotherm (BET) measurements (Tab. S1†). The scanning TEM (STEM) image and energy-dispersive X-ray spectrometry (EDS) mapping characterizations show that the $RuCl_3 \cdot 3H_2O$ are dispersed uniformly in the CAM complex, as shown in Fig. S1(d–h).† It is concluded that the higher the specific surface area by a stirring-calcination method, the more attachment sites exist for ruthenium coordination, thereby avoiding bulk aggregation during high-temperature calcination, promoting a highly uniform dispersion of ruthenium on the carbon matrix. As shown in Fig. 1(a), upon calcination at 550 °C, the Ru–CAM precursors could be carbonized into O-doped and N-doped carbon (CNO) with uniform Ru nanoparticles (NPs) through a pyrolysis route under the carbothermal reduction atmosphere of N_2. A large number of Ru nanoparticles are uniformly dispersed in the O-doped and N-doped carbon matrix. It could be definitely seen in Fig. 1(b) that the well-resolved lattice fringes with an interplanar spacing of approximately 0.21 nm are observed, which is consistent with the (101) plane of the high crystallinity of Ru (JCPDS No. 65-1863) seen *via* the high-resolution TEM image (HRTEM). The STEM image and EDS mapping characterizations shown through Fig. 1(c–f) further confirm that the Ru nanoparticles are dispersed in the carbon matrix uniformly.

As shown in Fig. 2(a), the X-ray diffraction (XRD) pattern of Ru/CNO-10 shows a series of characteristic peaks appearing at 38.3, 42.2, 44.0, 58.3, 69.4, 78.4, 84.7 and 85.9, which could be assigned to (100), (002), (101), (102), (110), (103), (112), and (201) planes of ruthenium, respectively, according to the XRD standard card (JCPDS No. 65-1863). The X-ray photoelectron spectroscopy (XPS) spectra demonstrate that the Ru/CNO-10 mainly contains Ru, C, N and O elements. In Fig. 2(b), the C 1s peak could be deconvoluted into three subpeaks at 284.5, 286.0, and 280.2 eV, which are assigned to sp^2 hybridization C=C, C=N, and the overlapped Ru $3d_{5/2}$ (Ru^0), respectively.[12] Simultaneously, the peaks appearing at 462.2 eV and 486.8 eV could be assigned to Ru $3p_{3/2}$ and Ru $3p_{1/2}$, respectively, in Fig. 2(c). As shown in Fig. 2(d), the peaks of N 1s appearing at 397.6 eV and 399.7 eV correspond to the C–N and N–H groups, respectively. The peaks appearing at 532.4 eV could be assigned to the C=O groups and 531.1 eV or 532.9 eV are possibly due to surface

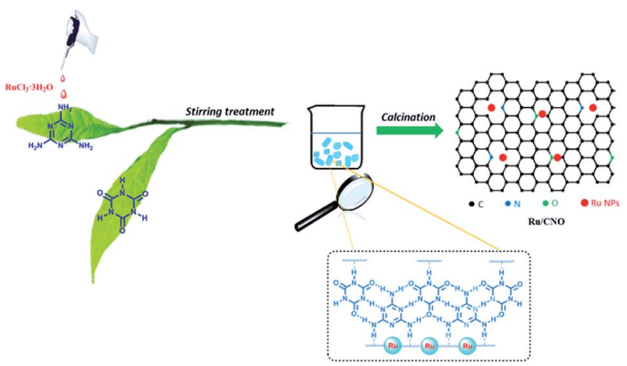

Scheme 1 Schematic of the synthesis of the Ru/CNO electrocatalysts.

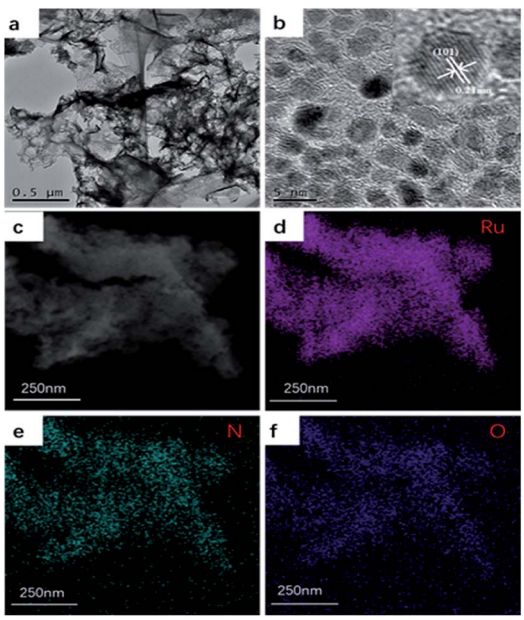

Fig. 1 (a) TEM images of Ru/CNO-10. (b) HRTEM image of Ru/CNO-10. (c) STEM-EDX mapping images of (d) Ru, (e) C, and (f) O in Ru/CNO-10.

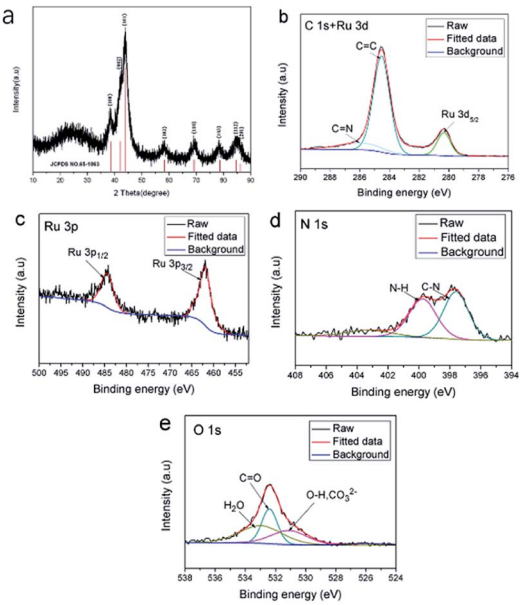

Fig. 2 (a) XRD pattern, (b) C 1s + Ru 3d, (c) Ru 3p, (d) N 1s and (e) O 1s spectra of Ru/CNO-10.

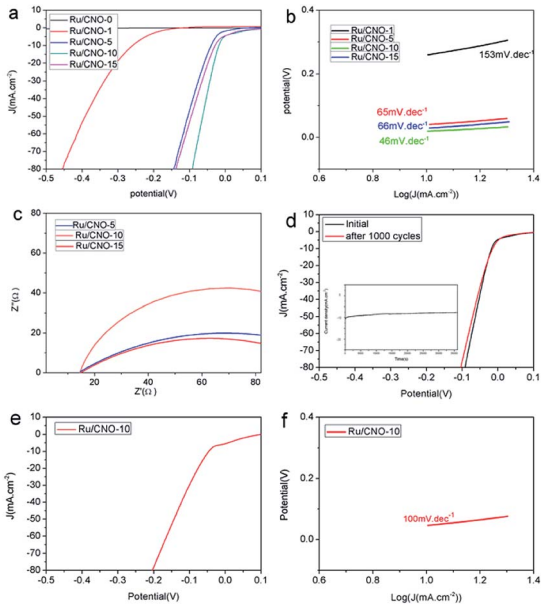

Fig. 3 (a) Polarization curves of Ru/CNO-0,1,5,10 and 15 in 0.5 M H_2SO_4. (b) Tafel plots of Ru/CNO-0,1,5,10 and 15 in 0.5 M H_2SO_4. (c) EIS Nyquist plots of Ru/CNO-5,10,15 at −300 mV in 0.5 M H_2SO_4. (d) Polarization curves of Ru/CNO-10 initially and after 1000 CV cycles in 0.5 M H_2SO_4. The inset shows the chronoamperometric response (i–t) of Ru/CNO-10 at a constant overpotential of −260 mV. (e) Polarization curves of Ru/CNO-10 in 1.0 M KOH. (f) Tafel plots of Ru/CNO-10 in 1.0 M KOH.

adsorbed oxygen-containing species such as H_2O, as shown in Fig. 2(e). All the experimental characterizations of TEM, XRD and XPS described above confirm the presence of uniform and highly-dispersed ruthenium nanocrystals on the N-doped and O-doped carbon matrix formed through the simple stirring-calcination process, which could help adjust the electronic properties of the adjacent atoms through an intramolecular charge transfer, resulting in promoting the hydrogen evolution reaction performance.

The electrochemical HER activities of Ru/CNO with different synthesis methods are further investigated in a 0.5 M H_2SO_4 solution. Compared with the grinding-calcination method and hydrothermal-calcination method, the HER catalytic performance indicates that the uniform ruthenium nanoparticles prepared by the simple stirring-calcination method at the calcination temperature of 550 °C has excellent catalytic activity, as shown in Fig. S2(a and b)†, which could be ascribed to ruthenium highly distributed on the nanorod materials before calcination. As shown in Fig. 3(a), it can be clearly seen from the polarization curves that the Ru/CNO-10 exhibits superior HER activity in the series of Ru/CNO materials synthesized by adding different amounts of $RuCl_3 \cdot 3H_2O$. When the current density is −10 mA cm^{-2}, the optimal Ru/CNO-10 electrocatalyst expresses a low overpotential of −18 mV and a low Tafel slope of only 46 mV dec^{-1} (Fig. 3(a and b)). At the current densities of −20, −50, −100 mA cm^{-2}, the overpotentials of Ru/CNO-10 are −32, −63 and −112 mV, respectively (Fig. S2(c)†). In addition, the electrochemical double-layer capacitance (C_{dl}) value of Ru/CNO-10 is 8.6 mF cm^{-2}, which is higher than Ru/CNO-0 (0.2 mF cm^{-2}) and Ru/CNO-5 (4.9 mF cm^{-2}), indicating that this material has a larger electrochemical surface area and could expose more electrochemically active sites (Fig. S2(d)†). The electrochemical impedance spectroscopy (EIS) images demonstrate that Ru/CNO-10 with the smallest semicircle radius has lower charge-transfer resistance (R_{ct}) than that of Ru/CNO-5 and Ru/CNO-15 (Fig. 3(c)). Simultaneously, the result of durability test shows an increase in overpotential of about −4 mV after 1000 cycles at −10 mA cm^{-2}, which could be attributed to some of the obvious sample peeling from the glassy carbon electrode after a long period of cycling (Fig. 3(d)). The long-term chronoamperometry (CA) test shows a slight activity degradation over 10 h, which further confirms the fact that Ru/CNO-10 is a stable electrocatalyst (Fig. 3(d)). It is known that due to the additional water dissociation step in an alkaline medium, HER often suffers from sluggish reaction kinetics so that many catalysts with good performance in acidic media could lose considerable activity in alkaline media. However, when the current density is −10 mA cm^{-2}, the optimal Ru/CNO-10 electrocatalyst expresses a low overpotential of −46 mV and a lower Tafel slope of 100 mV dec^{1} in 1.0 M KOH, as shown in Fig. 3(e and f), which indicates that Ru/CNO-10 electrocatalyst also shows excellent performance under alkaline media. In addition, along with the increase in relative current density, the Ru/CNO-10 electrocatalyst displays good stability in 1.0 M KOH.

3 Conclusions

In summary, we have revealed a simple route for the synthesis of Ru-based electrocatalysts with excellent HER performance under both acidic and alkaline conditions. The exceptional HER activity could be attributed to the Ru–CAM formed through

hydrogen-bond-driven self-assembly between melamine and cyanuric acid, which has a larger specific surface area and a great number of single-sites for the coordination of Ru with N and O, resulting in ruthenium precursors for subsequent annealing to be uniform ruthenium nanoparticles. This finding opens a new avenue for the application of the CAM self-assembly as an ideal strategy to construct uniform metal-based electrocatalysts with high HER performance *via* a series of highly dispersed metal–CAM precursors.

Conflicts of interest

There are no conflicts to declare.

Acknowledgements

This work was supported by the National Natural Science Foundation of China (21502012), the Chongqing Science and Technology Commission (cstc2017jcyjAX0404, cstc2017jcyjAX0116), the Scientific and Technological Research Program of Chongqing Municipal Education Commission (No. KJ1500615, KJ1706174), Chongqing Technology and Business University (2015-56-11, 1756002).

Notes and references

1 (*a*) T. R. Cook, D. K. Dogutan, S. Y. Reece, Y. Surendranath, T. S. Teets and D. G. Nocera, *Chem. Rev.*, 2010, **110**, 6474–6502; (*b*) N. Armaroli and V. Balzani, *Angew. Chem., Int. Ed.*, 2007, **46**, 52–66.

2 (*a*) W. Lubitz and B. Tumas, *Chem. Rev.*, 2007, **107**, 3900–3903; (*b*) G. Maggio, A. Nicita and G. Squadrito, *Int. J. Hydrogen Energy*, 2019, **44**, 11371–11384; (*c*) C. Acar and I. Dincer, *J. Clean. Prod.*, 2019, **218**, 835–849.

3 (*a*) C. G. Morales-Guio, L.-A. Stern and X. Hu, *Chem. Soc. Rev.*, 2014, **43**, 6555–6569; (*b*) N. Mahmood, Y. Yao, J.-W. Zhang, L. Pan, X. Zhang and J.-J. Zou, *Adv. Sci.*, 2017, **5**, 1700464; (*c*) Z. Chen, X. Duan, W. Wei, S. Wang, S. Wang and B.-J. Ni, *J. Mater. Chem. A*, 2019, **7**, 14971–15005; (*d*) G. Zhou, Y. Shan, L. Wang, Y. Hu, J. Guo, F. Hu, J. Shen, Y. Gu, J. Cui, L. Liu and X. Wu, *Nat. Commun.*, 2019, **10**, 399–406; (*e*) Y. Pan, K. Sun, S. Liu, X. Cao, K. Wu, W.-C. Cheong, Z. Chen, Y. Wang, Y. Li, Y. Liu, D. Wang, Q. Peng, C. Chen and Y. Li, *J. Am. Chem. Soc.*, 2018, **140**, 2610–2618; (*f*) F. Luo, Q. Zhang, X. Yu, S. Xiao, Y. Ling, H. Hu, L. Guo, Z. Yang, L. Huang, W. Cai and H. Cheng, *Angew. Chem., Int. Ed.*, 2018, **57**, 14862–14867; (*g*) J. Staszak-Jirkovský, C. D. Malliakas, P. P. Lopes, N. Danilovic, S. S. Kota, K.-C. Chang, B. Genorio, D. Strmcnik, V. R. Stamenkovic, M. G. Kanatzidis and N. M. Markovic, *Nat. Mater.*, 2016, **15**, 197–203.

4 (*a*) Q. Shao, F. Li, Y. Chen and X. Huang, *Adv. Mater. Interfaces*, 2018, **5**, 1800486; (*b*) Q.-Q. Yan, D.-X. Wu, S.-Q. Chu, Z.-Q. Chen, Y. Lin, M.-X. Chen, J. Zhang, X.-J. Wu and H.-W. Liang, *Nat. Commun.*, 2019, **10**, 4977–4985; (*c*) Y. Chen, S. Ji, W. Sun, Y. Lei, Q. Wang, A. Li, W. Chen, G. Zhou, Z. Zhang, Y. Wang, L. Zheng, Q. Zhang, L. Gu, X. Han, D. Wang and Y. Li, *Angew. Chem., Int. Ed.*, 2020, **59**, 1295–1301.

5 (*a*) J. Creus, J. D. Tovar, N. Romero, J. García-Antón, K. Philippot, R. Bofill and X. Sala, *ChemSusChem*, 2019, **12**, 2493–2514; (*b*) Z. Pu, I. S. Amiinu, Z. Kou, W. Li and S. Mu, *Angew. Chem., Int. Ed.*, 2017, **56**, 11559–11564; (*c*) F. Li, G.-F. Han, H.-J. Noh, I. Ahmad, I.-Y. Jeon and J.-B. Baek, *Adv. Mater.*, 2018, **30**, 1803676; (*d*) Y. Zheng, Y. Jiao, Y. Zhu, L. H. Li, Y. Han, Y. Chen, M. Jaroniec and S. Z. Qiao, *J. Am. Chem. Soc.*, 2016, **138**, 16174–16181; (*e*) J. Su, Y. Yang, G. Xia, J. Chen, P. Jiang and Q. Chen, *Nat. Commun.*, 2017, **8**, 14969–14978; (*f*) J. Mahmood, F. Li, S.-M. Jung, M. S. Okyay, I. Ahmad, S.-J. Kim, N. Park, H. Y. Jeong and J.-B. Baek, *Nat. Nanotechnol.*, 2017, **12**, 441–446; (*g*) C. Xu, M. Ming, Q. Wang, C. Yang, G. Fan, Y. Wang, D. Gao, J. Bi and Y. Zhang, *J. Mater. Chem. A*, 2018, **6**, 14380–14386; (*h*) J. Liu, G. Ding, J. Yu, X. Liu, X. Zhang, J. Guo, J. Zhang, W. Ren and R. Che, *J. Mater. Chem. A*, 2019, **7**, 18072–18080; (*i*) Y. Li, J. Abbott, Y. Sun, J. Sun, Y. Du, X. Han, G. Wu and P. Xu, *Appl. Catal., B*, 2019, **258**, 117952.

6 W. Li, Y. Liu, M. Wu, X. Feng, S. A. T. Redfern, Y. Shang, X. Yong, T. Feng, K. Wu, Z. Liu, B. Li, Z. Chen, J. S. Tse, S. Lu and B. Yang, *Adv. Mater.*, 2018, **30**, 1800676.

7 B. Lu, L. Guo, F. Wu, Y. Peng, J. E. Lu, T. J. Smart, N. Wang, Y. Z. Finfrock, D. Morris, P. Zhang, N. Li, P. Gao, Y. Ping and S. Chen, *Nat. Commun.*, 2019, **10**, 631–641.

8 (*a*) J. Wu, L. Xiong, B. Zhao, M. Liu and L. Huang, *Small Methods*, 2019, **3**, 1900540; (*b*) H. Liu, X. Peng and X. Liu, *ChemElectroChem*, 2018, **5**, 2963–2974; (*c*) J. Yang, B. Chen, X. Liu, W. Liu, Z. Li, J. Dong, W. Chen, W. Yan, T. Yao, X. Duan, Y. Wu and Y. Li, *Angew. Chem., Int. Ed.*, 2018, **57**, 9495–9500; (*d*) J. N. Tiwari, A. M. Harzandi, M. Ha, S. Sultan, C. W. Myung, H. J. Park, D. Y. Kim, P. Thangavel, A. N. Singh, P. Sharma, S. S. Chandrasekaran, F. Salehnia, J.-W. Jang, H. S. Shin, Z. Lee and K. S. Kim, *Adv. Energy Mater.*, 2019, **9**, 1900931; (*e*) Z.-L. Wang, K. Sun, J. Henzie, X. Hao, C. Li, T. Takei, Y.-M. Kang and Y. Yamauchi, *Angew. Chem., Int. Ed.*, 2018, **57**, 5848–5852; (*f*) J. Zhang, X. Xu, L. Yang, D. Cheng and D. Cao, *Small Methods*, 2019, **3**, 1900653; (*g*) C.-H. Chen, D. Wu, Z. Li, R. Zhang, C.-G. Kuai, X.-R. Zhao, C.-K. Dong, S.-Z. Qiao, H. Liu and X.-W. Du, *Adv. Energy Mater.*, 2019, **9**, 1803913; (*h*) S. Drouet, J. Creus, V. Collière, C. Amiens, J. García-Antón, X. Sala and K. Philippot, *Chem. Commun.*, 2017, **53**, 11713–11716.

9 B. Roy, P. Bairi and A. K. Nandi, *RSC Adv.*, 2014, **4**, 1708–1734.

10 (*a*) A. Ranganathan, V. R. Pedireddi and C. N. R. Rao, *J. Am. Chem. Soc.*, 1999, **121**, 1752–1753; (*b*) T. J. Prior, J. A. Armstrong, D. M. Benoit and K. L. Marshall, *CrystEngComm*, 2013, **15**, 5838–5843.

11 (*a*) D. Nagai and T. Kimoto, *RSC Adv.*, 2016, **6**, 103304–103310; (*b*) D. Nagai, T. Kuribayashi, H. Tanaka, H. Morinaga, H. Uehara and T. Yamanobe, *RSC Adv.*, 2015, **5**, 30133–30139.

12 S.-W. Sun, G.-F. Wang, Y. Zhou, F.-B. Wang and X.-H. Xia, *ACS Appl. Mater. Interfaces*, 2019, **11**, 19176–19182.

